RSC Advances

This article can be cited before page numbers have been issued, to do this please use: G. Marafon, D. Mosconi, D. Mazzier, B. Biondi, M. De Zotti and A. Moretto, *RSC Adv.*, 2016, DOI: 10.1039/C6RA17673A.

ROYAL SOCIETY OF CHEMISTRY

www.rsc.org/advances

Shaping bioinspired photo-responsive microstructures by the light-driven modulation of selective interactions

Giulia Marafon,[a] Dario Mosconi,[a] Daniela Mazzier,[a] Barbara Biondi,[b] Marta De Zotti,[a]* Alessandro Moretto[a,b]*

[a]Department of Chemical Sciences, University of Padova, 35131 Padova, Italy
[b]Institute of Biomolecular Chemistry, Padova Unit, CNR, 35131 Padova, Italy

e-mail: alessandro.moretto.1@unipd.it
e-mail: marta.dezotti@unipd.it

Abstract: A set of thymine-functionalized chromophores such as tetraphenylporphyrin, *azo*benzene and carbon quantum dots were synthesized and studied in terms of their self-recognition abilities to generate ordered nano-architectures. Additionally, fully adenine-capped, water soluble, gold nanoparticles were synthesized and properly characterized. In particular, even we observed a strong self-recognition between thymine-thymine systems, the fully functionalized adenine-capped nanoparticles act as a "breaking" molecular binder thus to allow the complementary recognition with the thymine-functionalized chromophores and the consequent molecular reorganization. It was found that adenine-thymine binding, occurring between these complementary self-organized complex systems, allowed the formation of precisely assembled nano-systems that powerfully depend in their morphologies from the nature of the chromophores utilized. These well-organized supramolecular architectures are able to undergo to morphologically self-shaping process under illumination by visible light, through the activation of the plasmon resonance of gold nanoparticles which selectively affected, and precisely rearranged, the binding modes of the self-assembled microstructures at the nanoscale level. Finally, these studies were extended to the selective molecular recognition at the surface, confirming the high binding affinity of these complex systems even at this level.

Introduction

The design and creation of bioinspired self-shaping microstructures represent a new way to develop shape-adaptation in synthetic materials. In distinction to shape-memory polymers, the self-shaping abilities in these bioinspired materials are located at the nanoscale, rather than the molecular, level.[1] In this view, self-assembly can be considered as the most powerful autonomous organization of components able to produce structures at any scale level, and this phenomenon takes part in many essential biological, chemical, and physical processes. In these complex systems, the self-organization is synergically driven by specific intermolecular interactions, like π-π stacking interactions, hydrogen bonds, electrostatic interactions, hydrophobic forces.[2-4] Nowadays, following the bio-inspiration concept, many new types of functional materials are readily achieved through the selective molecular recognitions between defined componets.[5-9] One of the most important examples of realization of highly selective molecular process in Nature is the mutual recognition of complementary nucleobases by means of the selectivity, directionality, reversibility, and cooperativeness of hydrogen bonds.[10-14] While the Watson–Crick base pairing is dominant within nucleic acids constrained by the geometry of the double helix, it is important to note that the nucleobases linked to synthetic systems may change their binding behaviour.[15] Thus, reverse Watson–Crick, Hoogsteen, 'wobble' base pairs and other nucleobase binding modes play important roles in any artificial-nucleobase self-assembly process mainly controlled by its hydrogen bonding network.[16] Furthermore, in the hybrid-nucleobase systems the chemical nature of the linked molecules play, additionally, an important role in self-assembly process. Finally, hydrogen-bonding interactions alone cannot yield significant driving forces for molecular recognition in bulk water due to the strong competitive binding of water molecules.[17] In this perspective, a prior design of the directional mode of complementary hydrogen-bonding may overcome the competition of the aqueous environment and the self-recognition antagonism between the same type of nucleobases.[18] In this work we report the selective adenine-thymine binding occurring between complementary self-organized complex systems, such as gold nanoparticles, with suitable functionalized

View Article Online
DOI: 10.1039/C6RA17673A

chromophores, such as *tetra*phenylporphyrin, *azo*benzene and carbon quantum dots (CQDs),[19] that resulted in well-organized supramolecular architectures. Importantly, we reported three examples of governable morphological transition process, induced by the light activation of the plasmon resonance of the gold nanoparticles.

Results and Discussion

Synthesis of thymine- and adenine-functionalized chromophores

The chemical structures of functionalized molecules reported in this work are presented in Fig. 1. Briefly, thymine was first converted in its corresponding acetic acid derivative, namely thymine-1-acetic acid,[20] while adenine was converted in its acetic ethyl ester derivative, namely ethyl adenine-9-acetate (see SI).[21] Then, thymine-1-acetic acid was coupled either (i) with 5-(4-aminophenyl)-10,15,20-triphenyl porphyrin and subsequently converted in its metallated Zn-form, yielding **1** (Fig. 1, see SI), (ii) with 4-amino*azo*benzene, yielding **2** (Fig. 1, see SI) and (*iii*) amino-doped CQDs,[19,22-24] yielding **3** (Fig. 1, see SI). Ethyl adenine-9-acetate was converted in its mono-acetyl ethylen-diamino amide derivative and subsequently coupled with racemic lipoic acid, yielding **4** (Fig. 1, see SI). Compounds **1**-**3** were chemically (see SI) and spectroscopically characterized as illustrated in Fig. 2.

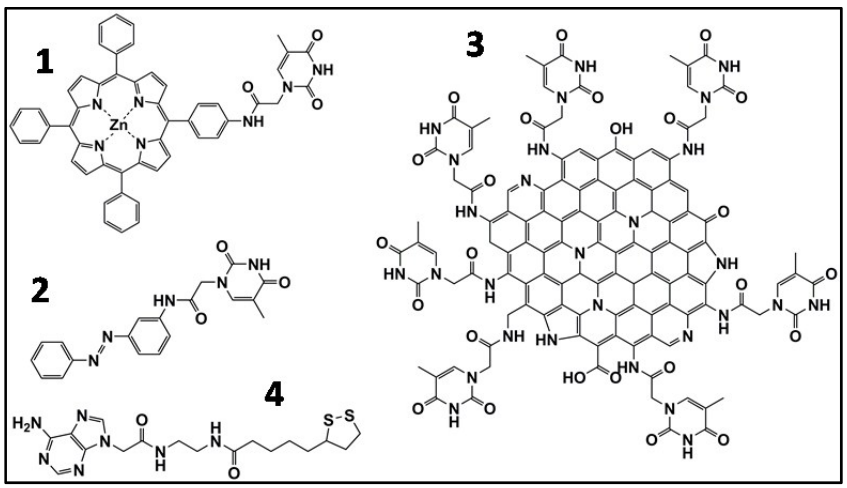

Fig. 1 Representation of the chemical structures of the compounds synthesized and studied in this work.

View Article Online
DOI: 10.1039/C6RA17673A

Fig. 2A shows a comparison of the UV-Vis absorption spectra of **1** (red line) and its non-metallated form (black line) in tetrahydrofuran (THF) solution. The two spectra exhibit the characteristic UV-Vis profiles of metallated porphyrin and porphyrin, respectively.[25] Fig. 2B displays the UV-Vis profiles of **2** recorded after three cycles of irradiation (at 350 or 420 nm) that reveals the reversible isomerization process occurring between the *trans* and *cis* forms.[26] This phenomenon was additionally investigated by ^{1}H-NMR as reported in SI. In this case, the chemical shifts of the protons belonging to the thymine part of the molecule are affected by the photoinduced isomerization process.

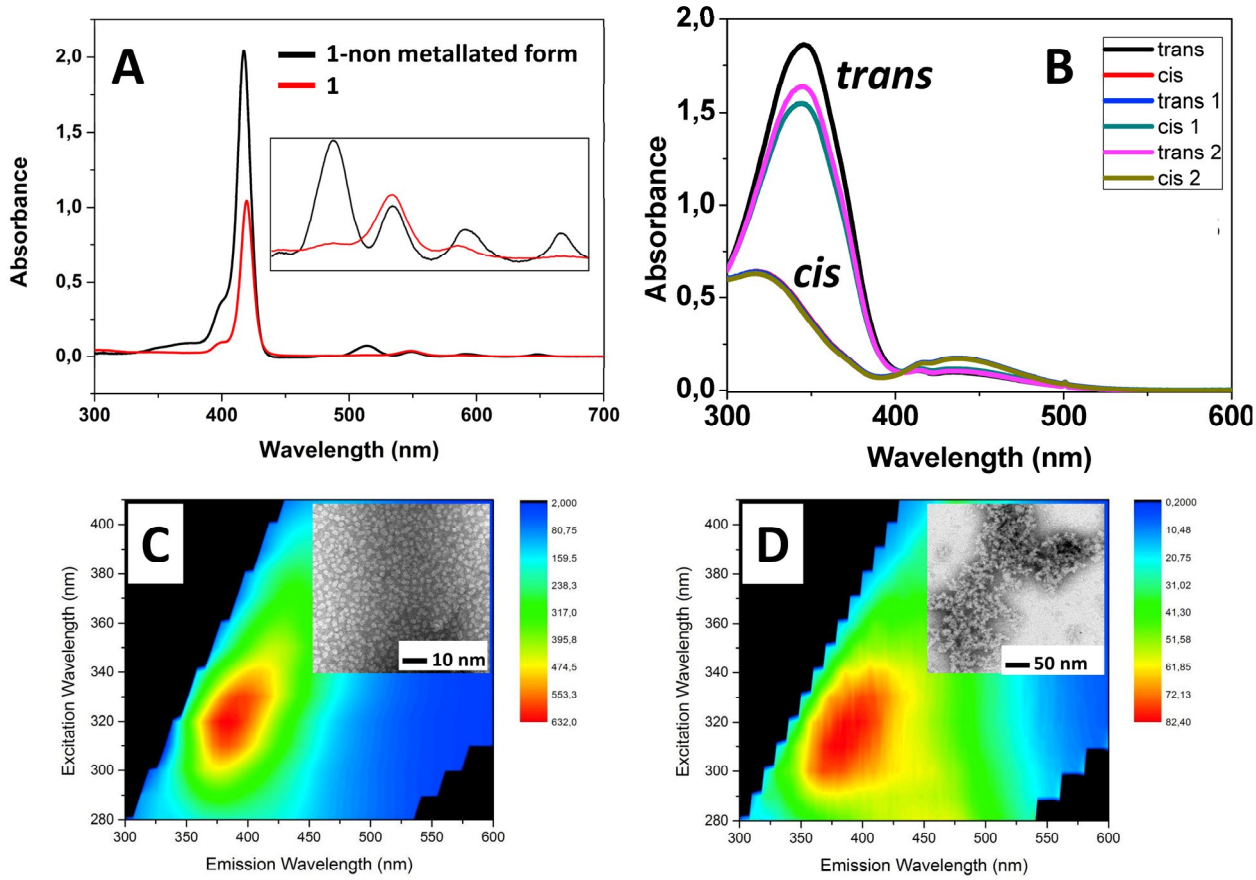

Fig. 2 (**A**) UV-Vis absorption spectra recorded for **1** (red line) and its non-metallated analog (black line) in a THF solution. (**B**) UV-Vis absorption spectra of a THF solution of **2** recorded after three complete irradiation cycles with light at 350 and 420 nm. (**C**) Fluorescence 2D spectrum recorded for pristine CQDs. Inset: TEM image of pristine CQDs. (**D**) Fluorescence 2D spectrum recorded for **3**. Inset: TEM image of **3**.

View Article Online
DOI: 10.1039/C6RA17673A

The comparison of the FT-IR absorption spectra recorded for pristine CQDs and **3** was the first evidence to confirm the occurrence of the chemical modification of pristine CQDs after coupling with thymine-1-acetic acid (see SI). Successively, Figs. 2C-D illustrates a comparison of TEM analyses and fluorescence spectra of pristine CQDs[23] and **3**, respectively. In particular, TEM analyses (Figs. 2C-D, inserts) revealed the formation of strongly aggregates structures occurring for **3** (probably resulting from thymine self-recognition). Importantly, as shown from a comparison of the fluorescence experiments (recorded in MeOH solution, Fig. 2D, right), the multi-color emission properties (taking place for pristine CQDs) are preserved in **3**.

Self-aggregation studies

A part of this work was devoted to the study of the self-aggregation properties of compounds **1-3** that may arise from thymine-thymine self-recognition.[27, 28] To this aim, compound **1** was dissolved in THF. Upon addition of water to the THF solution, flakes-like structures were recovered after few hours, as shown in Figs. 3A-B.

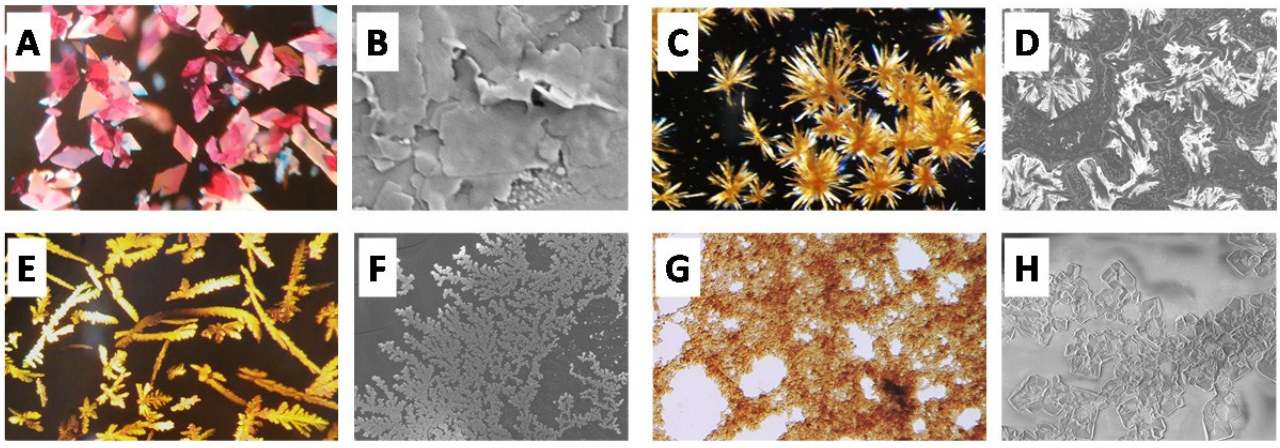

Fig. 3 (**A**) Optical microscope and (**B**) SEM images showing organized microstructures obtained from **1**. (**C,E**) Optical microscope and (**D,F**) SEM images revealing different structures adopted by **2** in its *trans* and its *cis* forms, respectively. (**G**) Optical microscope and (**H**) SEM images showing organized microstructures obtained from **3**.

View Article Online
DOI: 10.1039/C6RA17673A

Compound **2** was examined in its *trans* and *cis* conformers. Interestingly, it was found that slow evaporation from a THF/MeOH (methanol) solution provided different microstructure morphologies for the *trans* and the *cis* isomers (Figs. 3C-D, *trans* isomer, and Figs. 3E-F, *cis* isomer). Finally, slow evaporation from a water solution of **3** provided formation of ordered microstructures as shown in Figs. 3G-H. It is worth noting that the same experiments repeated for 5-(4-aminophenyl)-10,15,20-triphenyl porphyrin, *trans* 4-amino*azo*benzene and *cis* 4-amino*azo*benzene and pristine CQDs did not produce any type of microstructures. With these set of self-recognition experiments we demonstrated the strong aptitude of functionalized thymine to bind itself in a mixed THF/water solution.

Synthesis of adenine-capped gold nanoparticles

Then, nanometric-sized GNPs (**5**) covered by **4** (Fig. 4A) were synthesized. **4** was combined with tetrachloroauric acid in THF, and after an appropriate time of complexation the mixture was rapidly reduced by adding $NaBH_4$.[29] After 48 h aging, GNPs were recovered by filtration and fully characterized using transmission electronic microscopy (TEM), UV-Vis absorption spectroscopy, thermogravimetric analyses (TGA), and dynamic light scattering (DLS). From TEM images (sample dissolved in water), it was possible to highlight the strong self-aggregation tendency of this nanosystem, due to self-recognition mediated by intermolecular hydrogen bonds occurring among the adenine moieties (Fig. 4B). By using a DMSO/water mixture, it was possible to reduce the self-aggregation propensity and to detect a distribution of single GNPs (Fig. 4C). In Fig. 4D, the graph displays the narrow size distribution centered at a diameter of 1.5 nm observed for GNPs. The UV-Vis absorption spectrum of a diluted solution of nanoparticles in water resemble closely that of GNPs with a size lower than 2 nm, as confirmed by the presence of a slightly pronounced plasmonic resonance located at 520 nm (Fig. 4E). TGA analyses revealed a chemical composition of 42% of organic part and 58% of inorganic part (Fig. 4F). Thus, the number of Au atoms in the corresponding GNPs can be calculated from the dimension of the metallic core observed by TEM

View Article Online
DOI: 10.1039/C6RA17673A

images taking into account the density of bulk gold metal (55 atoms/nm^3, if a spherical model is applied).

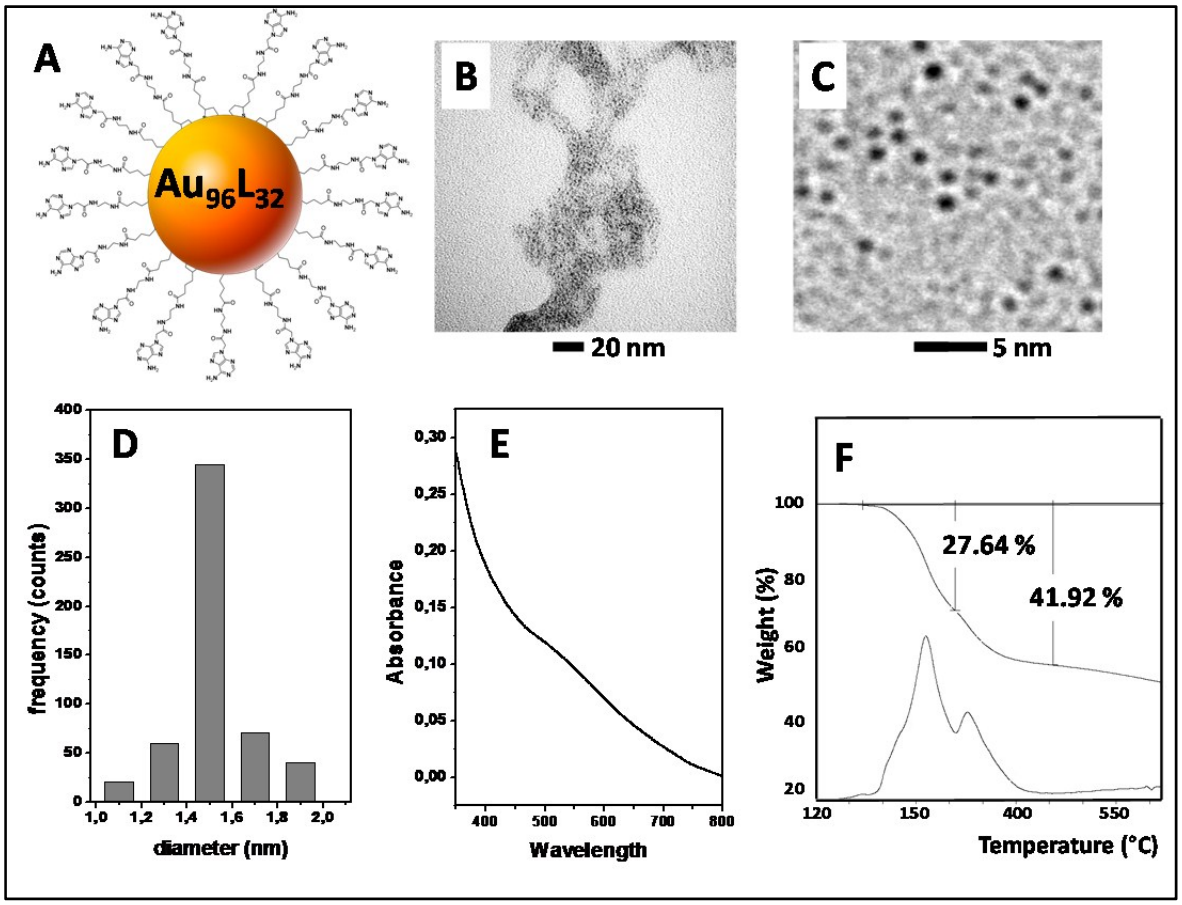

Fig. 4 (**A**) Schematic representation of adenine-capped GNPs. (**B**) TEM image of self-aggregated adenine-capped GNPs. (**C**) TEM image of dispersed adenine-capped GNPs. (**D**) Size distribution graph obtained considering a large number of dispersed adenine-capped GNPs. (**E**) UV-Vis absorption spectrum of adenine-capped GNPs dissolved in a DMSO/water mixture. (**F**) TGA analyses run on a solid sample of adenine-capped GNPs.

The number of adenines conjugated to the inorganic cluster was calculated from the TGA weight loss (corresponding to the weight fraction of the organic coating monolayer on the inorganic cluster) divided by the molecular weight of the related adenine conjugated to the inorganic core.[30] From all this information, we may estimate that the average chemical formula for these GNPs would be $Au_{96}L_{32}$. This formula is in good agreement with that of similarly sized GNPs resolved by X-ray crystallographic analyses that revealed a closely related number of gold atoms for a very

similar core size diameter, but concomitantly displayed a larger number of organic ligands.[31] In this connection, it is worth emphasizing that we used the disulfide-containing lipoic acid, which affords a double number of sulfur atoms for molecular unit (if compared to that of the GNPs resolved by X-ray crystallographic analyses). Thus, a lower number of ligands is required to passivate the gold core. From DLS measurements of a diluted water solution of adenine-capped GNPs, an average diameter of 6.5 nm *per* GNP was found (Fig. 5A). This value is in agreement with a hypothetic structure where the organic ligands (**4**) are placed in a fully-extended conformation.

Molecular recognition between adenine-capped GNPs and thymine-functionalized chromophores

By mixing a solution composed by **5** and **1**, a step toward a molecular recognition process mediated by thymine/adenine interactions was carried out. The basic idea is to detect a molecular recognition through formation of a double sized nanoparticle (with an estimated diameter of 11 nm, considering an extended conformation taking place for both **1** and **4**), which may result from the selective interaction of the adenine layer of the GNPs and **1** (Fig. 5B). To run this experiment, **5** was first dissolved in water and subsequently an equivalent of **1** (referred to the adenine ligand) was added from a high diluted THF solution (see SI for experimental details). After a mixing time of 24 h at 30 °C, a large number of single monomeric **1**/**5** nanosystems of 10-nm diameter were detected by DLS experiments (Fig. 5B) and TEM analyses (Fig. 5C). It is worth noting that the presence of the Zn^{2+} ion inside the porphyrin ring allowed detection of the 10 nm assembled nanoparticle core, which occurred in this case, by TEM. By both the techniques also a small amounts of large round aggregates were detected. With the aim to understand the origin of such large spherical microstructure aggregates we repeated the above described experiment keeping constant the number of GNPs and **1** equivalents but varying the concentration. In particular, after a slow addition of a THF solution of **1** to a water solution (20-time concentrated with respect to the previously reported experiment) of adenine-capped GNPs solution turned slightly opaque, and only large **1**/**5** nanosystems of 160 nm diameter were almost quantitatively detected by TEM analyses (Fig. 5D

View Article Online
DOI: 10.1039/C6RA17673A

and 5E) and DLS experiments (Fig. 5B). Since by TEM analyses it was hard to distinguish the presence of adenine-capped GNPs, we repeated the self-assembly experiment by using **1** in its non-metallated form.

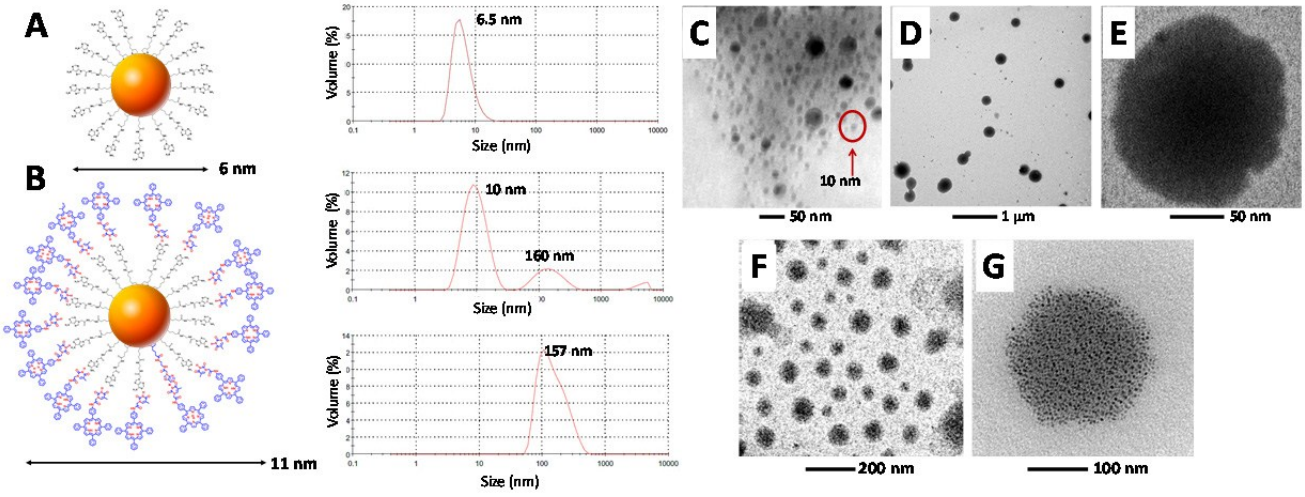

Fig. 5 (**A-B**) Representation and DLS analysis of **4**-capped GNPs and **4**-capped GNPs mixed with **1**, respectively. (**C**) TEM image showing monomeric, self-recognized **1**/adenine-capped GNPs. (**D**) TEM images showing a large view of **1**/adenine-capped GNPs self-assembled nanosystems. (**E**) TEM image showing a detailed view of a single aggregate. (**F**) TEM images showing a large view of **1** (in its non metallated form)/adenine-capped GNPs self-assembled nanosystems. (**G**) TEM images showing a detailed view of **1** (in its non metallated form)/adenine-capped GNPs nanosystems.

Also this case the TEM analyses confirmed the exclusive formation of large spherical aggregates (Fig. 5F) and moreover, from a detailed view of a single spherical aggregate (Fig. 5G) it was possible to distinguish singles **5** nanosystems that are not aggregated each-other, but rather they seem precisely spatially located within the aggregate. Because TEM analyses were run under ultra-high vacuum conditions, atomic force microscopy (AFM) (Fig. 6A) and environment scanning electron microscopy (E-SEM) (Fig. 6B) analyses were carried out on the large **1**/adenine-capped GNPs nanosystems, to provide more detailed morphological information under wet-like conditions.

By both techniques, formation of spherical-shaped aggregates, with similar dimensions of those observed by TEM, was detected. To understand the origin of these spherical superstructures, that could be related to the onset of a set of cooperative non-covalent bonds mediated by hydrogen bonding, π-π stacking and hydrophilic/hydrophobic interactions, we carried out UV-Vis absorption measurements. The UV-Vis absorption spectrum of **1**, recorded in THF, exhibits an intense Soret band at 419 nm, together with two weaker Q-bands at 547, and 587 nm (Fig. 6C, red line). In contrast, in the UV-Vis absorption spectrum of the spherically-shaped aggregates obtained, the Soret band is red-shifted to 429 nm, while the frequency of the two Q-bands falls at longer wavelengths, at 561 and 600 nm (Fig. 6C, black line, insert). The red-shift of the absorption bands of **1** indicates the formation of J-aggregates (Fig. 6D) .[32]

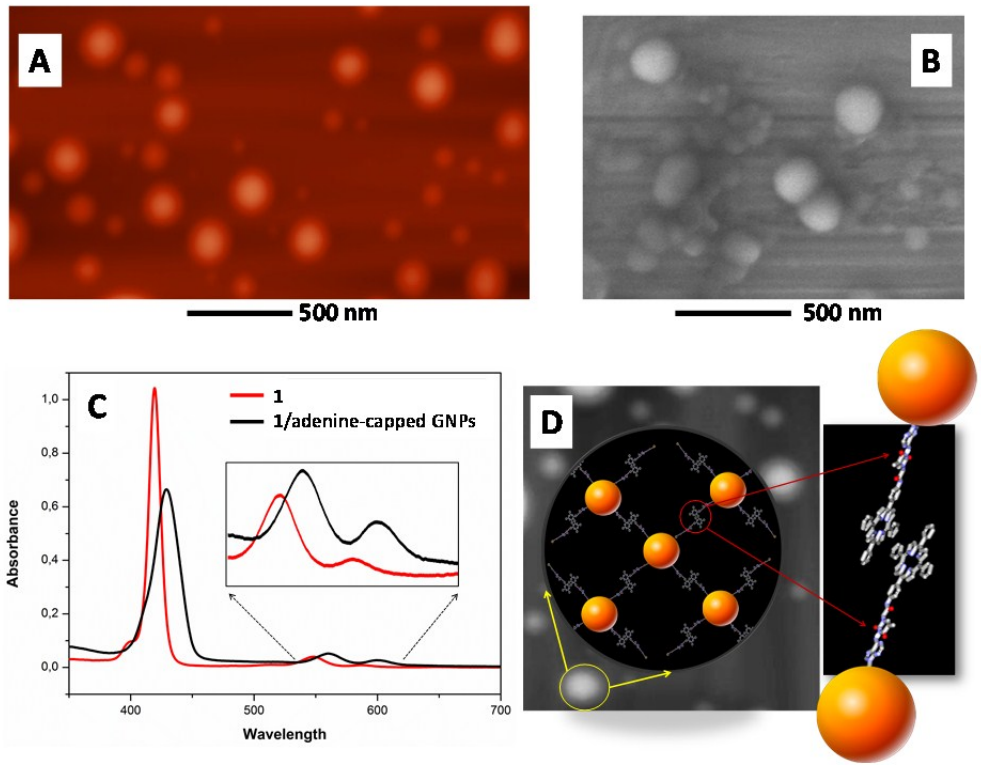

Fig. 6 (**A-B**) AFM and E-SEM images, respectively, showing a large view of **1**/adenine-capped GNPs self-assembled nanosystems. (**C**) UV-Vis absorption spectra in THF of **1** (red line) and **1**/adenine-capped GNPs (black line) self-assembled nanosystems. (**D**) Schematic representation of the hypothetic bulk network interactions occurring for these assembled nanosystems.

View Article Online
DOI: 10.1039/C6RA17673A

We decided to use light a 500 nm to promote an eventually occurring molecular reorganization. The principle is that at this wavelength the gold core of GNPs absorbs light, thus the resulting vibrational energy (heat) may flow from the gold core[33] across the adenine capping layer following excitation of the nanoparticle plasmon resonance, and finally could affected the adenine/thymine binding mode with consequence extended to the spatial distribution of the overall self-assembled systems (Fig. 7). Thus, we irradiated a solution of large spherical aggregates by using a LED at 500 nm. Under illumination, the opaque solution turned as a suspension after few minutes and this suspension was analysed directly by TEM. Fig. 3A (TEM under stained) displayed the occurred morphological transition from large spherical to straight fibers structures, while Fig. 3B (TEM under non-stained) showed the details of the nanoparticle disposition within the fibers structures.

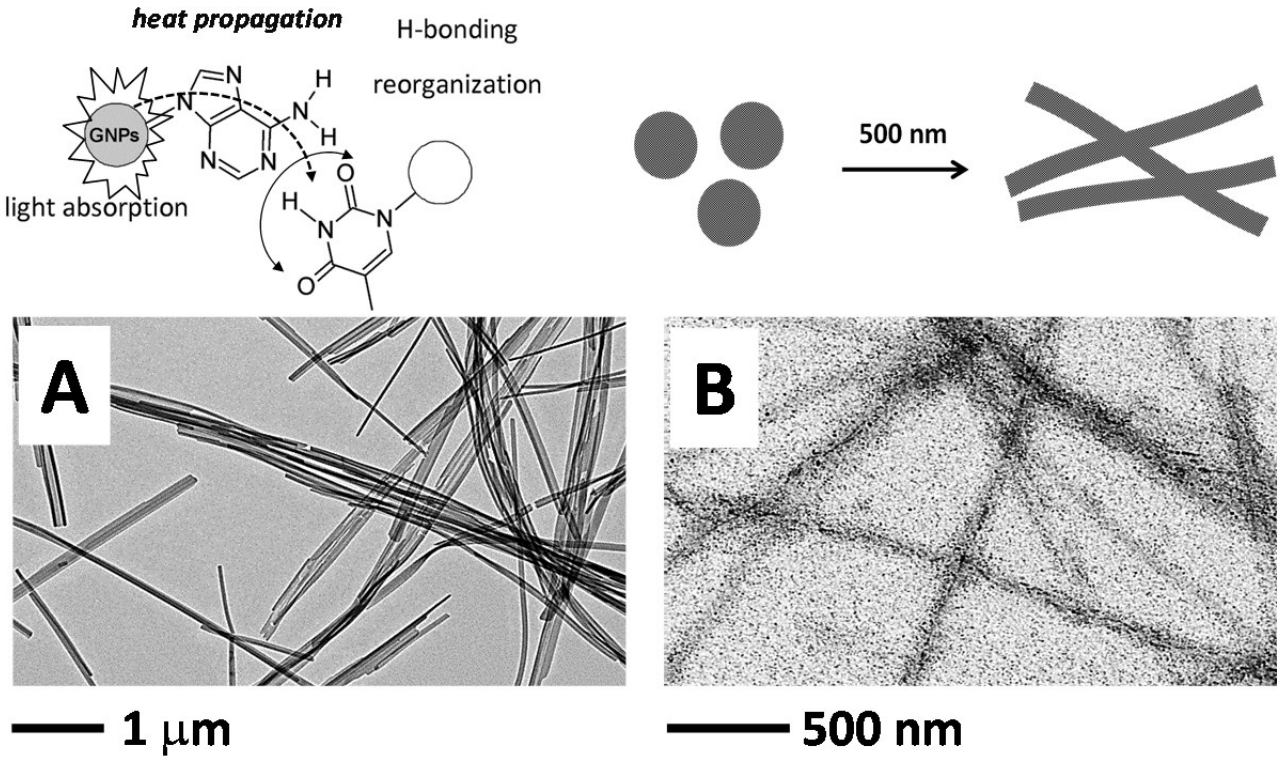

Fig. 7 (Upper part) Schematic representation of the light induced activation of the microstructure transition occurring in **1**/**5** self-assembled system. (**A**) TEM images (stained) showing the formation of fibers. (**B**) TEM images (non-stained) showing the GNPs within the fiber network.

View Article Online
DOI: 10.1039/C6RA17673A

As a control experiments, we used LED at different wavelengths (405, 465 and 585 nm), and under these condition no microstructures transition were found. We repeated the same type of experiment by mixing together **5** and **2** under the above experimental conditions. Interestingly, in the case of **2** in its *trans* form, a rapid formation of a suspension of straight fiber networks was observed after mixing the two components, as detected by SEM (Figs. 8A-B). Additionally, the same sample was further characterized by TEM (Figs. 8C-D, under stained and non-stained conditions, respectively) which revelled the spatial arrangement of the GNPs inside the novel microstructure formed. Moreover, after a prolonged irradiation at 365 nm (*trans* to *cis azo*benzene isomerization), the previous suspension was converted in a milk-like suspension, that resulted as a dense network of bent fibers, as detected by SEM (Figs. 8E-F).

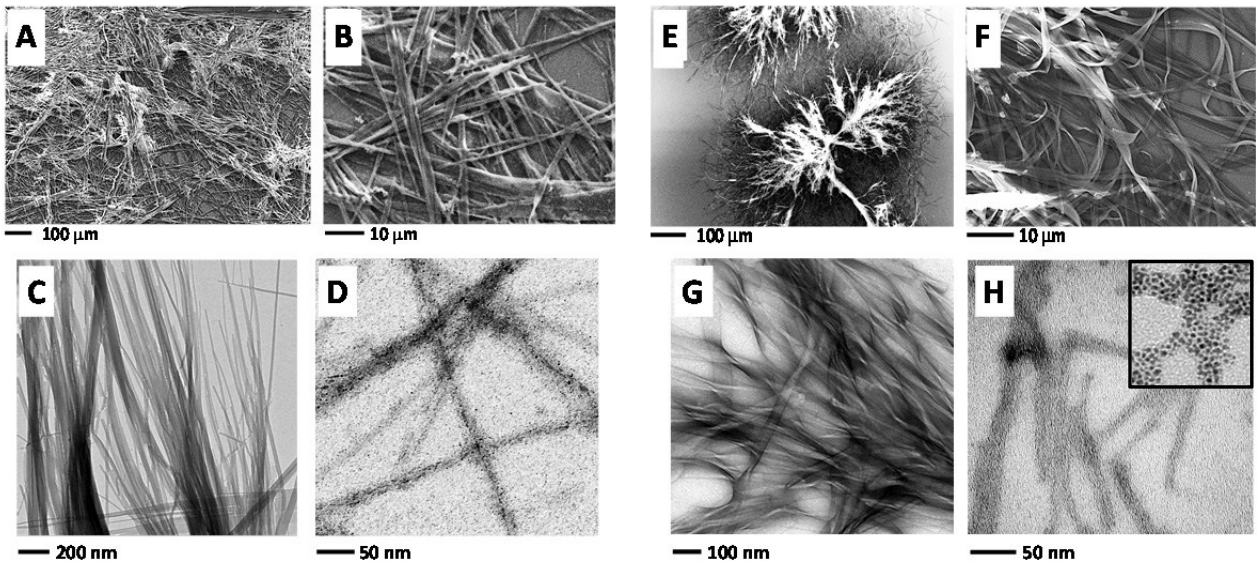

Fig. 8 (**A-B**) SEM images showing formation of microstructures composed of straight fibers network, occurring by mixing **2** (in its *trans* form) with adenine-capped GNPs. (**C-D**) Corresponding TEM images, stained and un-stained respectively, showing the fiber type nature of the network, and highlighting adenine-capped GNPs inside the fibers. (**E-F**) SEM images showing the formation of novel microstructures composed of dense network of bent fibers, after irradiation at 350 nm of the "*trans*" microstructures (**2** is in its *cis* form). (**G-H**) Corresponding TEM images, stained and un-stained respectively, showing the fiber type nature of the network, and highlighting details the GNPs within the fiber network.

View Article Online
DOI: 10.1039/C6RA17673A

The same sample was further characterized by TEM (Figs. 8G-H, under stained and non-stained conditions, respectively) and the results confirmed the bent morphology adopted by this supramolecular system under light exposure, and highlighted the presence of adenine-capped GNPs inside the fiber networks. The possibility to convert the straight fiber network into a bent fiber network by a photo-induced process suggested that the *azo*benzene moieties are not densely packed within the fiber network, so that they are able to isomerize, under irradiation, between their *trans* and *cis* forms. Moreover, the isomerization process seems not to affect recognition with the nanoparticles, but rather it appears to act only on the directional propagation of the resulting fibers. Moreover, after irradiation by LED at 500 nm of the bent fibers network, bunch-like microstructure were readily obtained (Fig. 9A stained, and Fig. 9B non-stained, conditions).

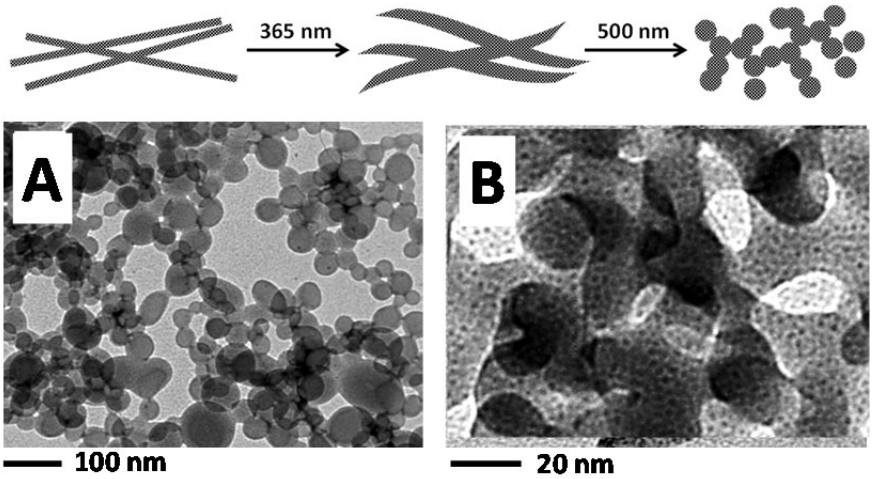

Fig. 9. (**A**-**B**) TEM images showing detail of bunch-like microstructure(stained) and details the GNPs within the bunch-like network, respectively.

Finally, this approach was extended to **3** with the aim at obtaining branched structures due to the multivalent nature of both components, thymine-functionalized CQDs and adenine-capped GNPs. Surprisingly enough, the resulting mixture appeared as a transparent solution even under different *w*/*w* ratios of **3**/adenine-capped GNPs (both mixed from mother water solutions). We found that the

View Article Online
DOI: 10.1039/C6RA17673A

photoemission activities of the resulting mixtures were still, but with a significant intensity decrease, present (Fig. 10A).

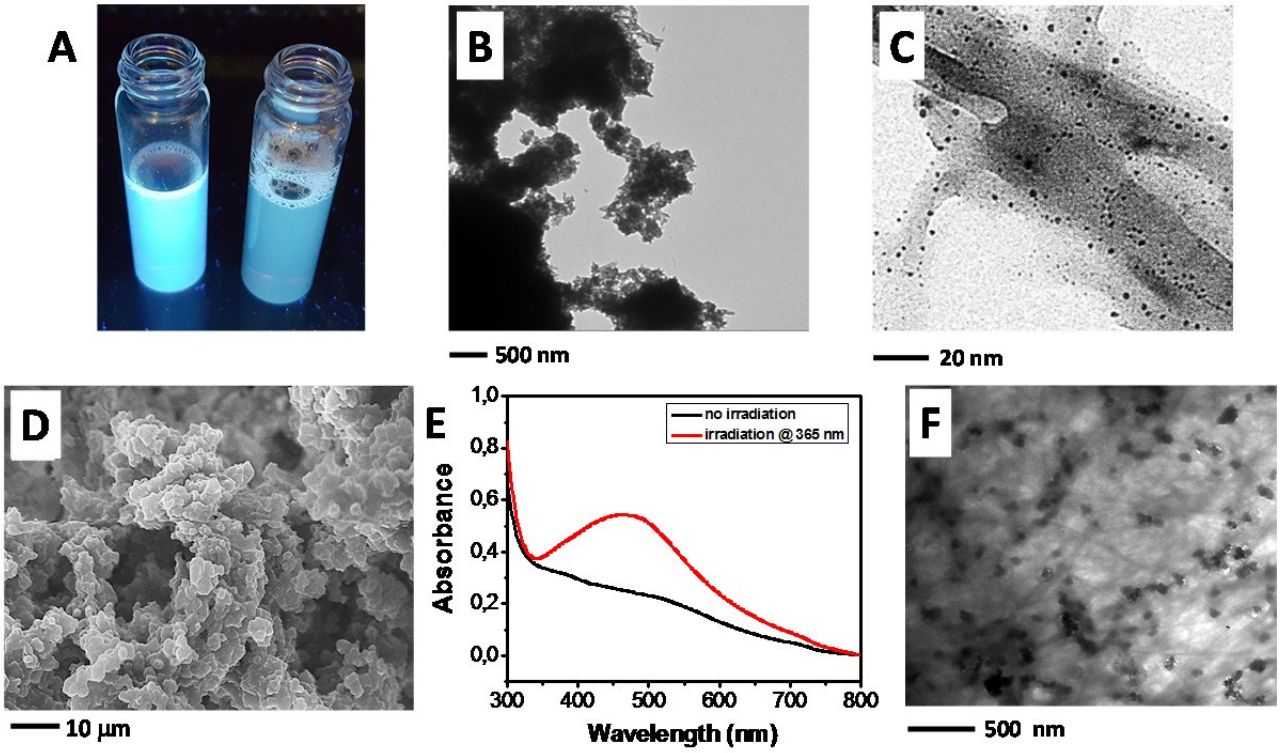

Fig. 10 (**A**) Pictures showing a **3** solution in water (left) and a **3**/adenine-capped GNPs water mixture (right) under exposure of light at 365 nm. (**B**) TEM image (stained) recorded from the **3**/adenine-capped GNPs water mixture showing the formation of aggregates. (**C**) TEM image (non-stained) recorded from the **3**/adenine-capped GNPs water mixture showing the presence of adenine-capped GNPs within the aggregate.(**D**) SEM image of the solid material collected from a 4:1 *w*/*w* ratio of the **3**/adenine-capped GNPs mixture. (**E**) UV-Vis absorption spectra recorded before and after irradiation at 365 nm. (**F**) TEM image showing formation of large Ag clusters.

These mixture were further examined by TEM and the results from these analyses displayed the formation of large aggregate (Fig. 10B, under stained condition). The TEM measurements under non-stained condition (Fig. 10C) shown the disposition of the adenine-capped GNPs inside the aggregate. Thus, formation of solid aggregates was forced by slow diffusion of THF vapors to these water solutions. In all cases, we observed formation of "swelled-type" precipitates that were collected, allowed to dry under ambient conditions, and morphologically analyzed by SEM. In

View Article Online
DOI: 10.1039/C6RA17673A

particular, Fig. 10D reports the morphological characterization of the material collected from a 4:1 *w*/*w* ratio of the **3**/adenine-capped GNPs mixture, which proved the occurrence of a uniform sponge-like morphology for this sample. We exploited the electron-donating capabilities of photoexcited CQDs, which eventually enable reduction of silver salts to the corresponding AgNPs on the surface of the CQDs themselves. [24] A water solution of silver nitrate was directly mixed with a 4:1 *w*/*w* ratio of the **3**/adenine-capped GNPs mixture. After the slow diffusion of THF vapors to this mixture, the "swelled-type" precipitate was collected and allowed to dry on a thin glass support. This material was directly photoexcited with UV light (365 nm) over a period of 1 h. Formation of AgNPs within the resulting material was confirmed by UV-Vis absorption spectroscopy, *via* the detection of a strong Ag plasomic resonance, and by TEM analyses (Figs. 10E-F). Additionally, after irradiation by LED at 500 nm of the swelled-type precipitate (Fig. 11A), flat-like microstructures were obtained (Figs. 11B-C) as shown by TEM analyses.

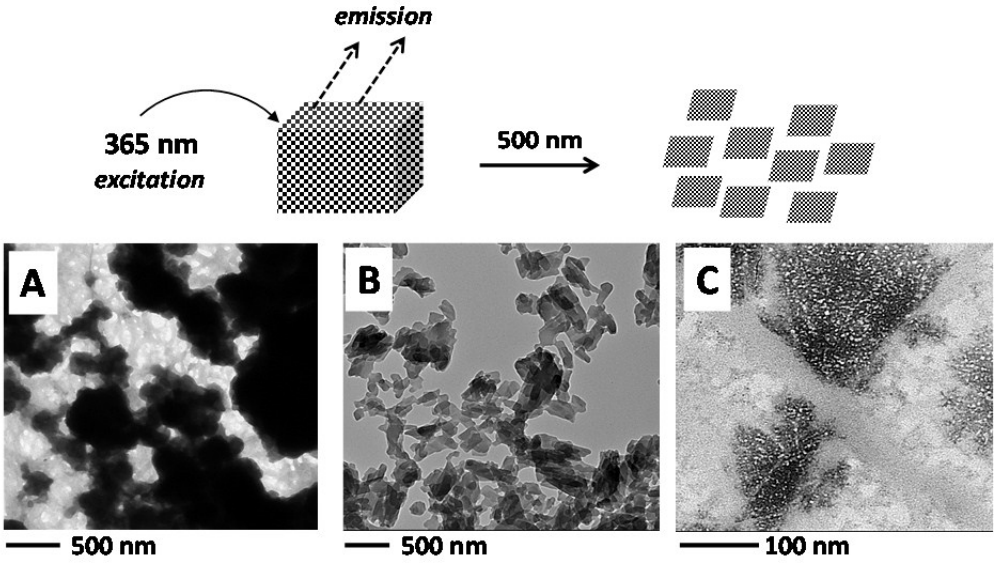

Fig. 11 (Upper part) Schematic representation of the light induced activation in **3**/**5** self-assembled system: (i) photoemission occurring using light at 365 nm and (ii) microstructure transition using light at 500 nm (**A**) TEM image of the bulk material. (**B**-**C**) TEM images of flat microstructure (stained) and of GNPs within the flat microstructure (non-stained), respectively.

Molecular recognition on polymer support

Once we proved the occurrence of selective recognition between functionalized adenine and thymine, we expanded our studies on this phenomenon at the surface level. To this purpose, we used a thiol functionalized polymer that is readily accessible by a two-component thiol-ene chemistry polymerization, between a 2,4,6-triallyloxy-1,3,5-triazine and 2,2′-(ethylenedioxy)diethanethiol. The resulting gummy-like highly, cross-linked polymer (Figs. 12A-B, and see SI for details) presents a large number of free thiols on its surface, and it is spectroscopically transparent to light above 390 nm (Fig. 12D, blue line). We took advantage of these free thiol groups to anchor **4**-capped GNPs to the polymeric matrix *via* a thiol-to-thiol exchange reaction (Fig. 12A).

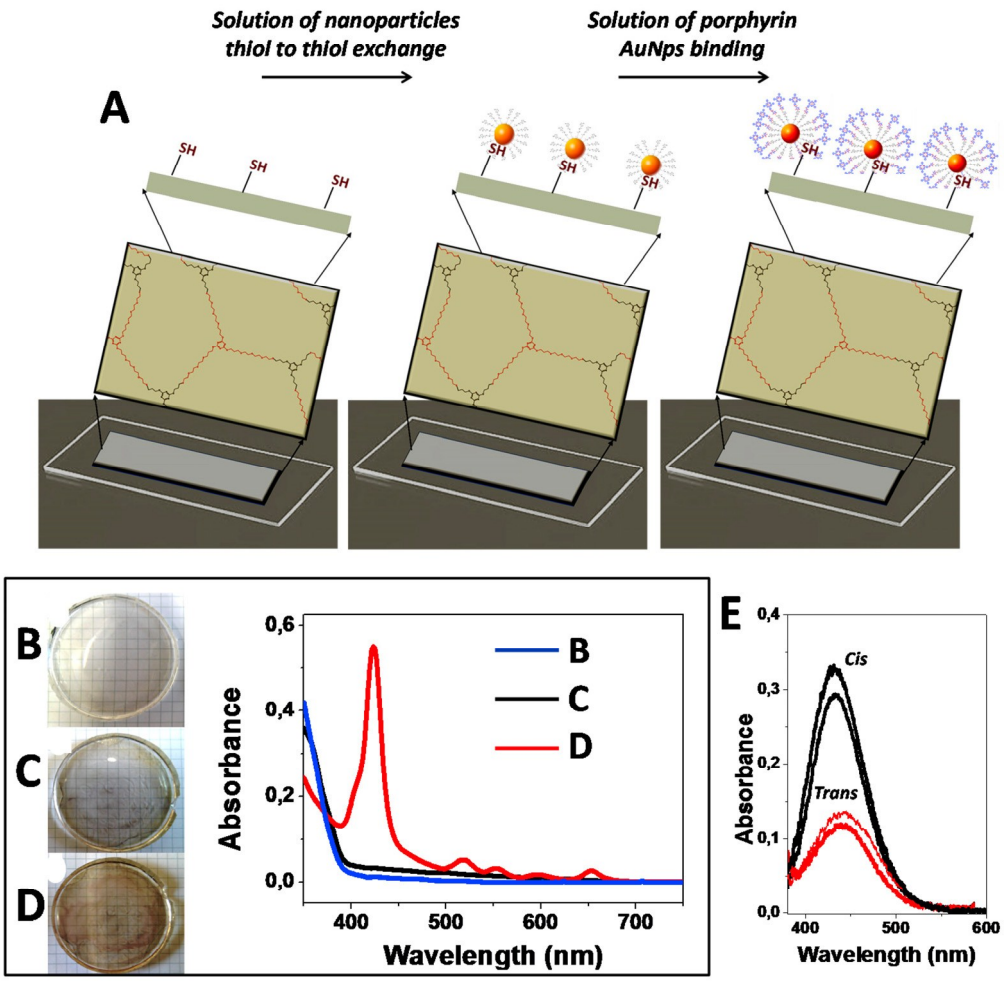

View Article Online
DOI: 10.1039/C6RA17673A

Fig. 12 (**A**) Schematic representations of the surface binding experiments occurring over the thiol-functionalized polymer (left), by using **4**-GNPs (center), and **1** in its non-metallated form (right). **(B-D)** Pictures showing, respectively, the thiol-functionalized polymer, the **1**-GNPs/functionalized polymer, and the **1**-GNPs/functionalized polymer and the corresponding solid-state UV-Vis absorption spectra recorded for: thiol-functionalized polymer (blue line), **4**-GNPs/functionalized polymer (black line), and **1** (in its non-metallated form)/**4**-GNPs/functionalized polymer (red line). (**E**) Solid-state UV-Vis absorption spectra recorded during three reversible cycle of isomerization (*cis*/*trans*) occurred directly on **2**/**4**-GNPs/functionalized polymer surface, by using light at 365 or 420 nm

The resulting slightly colored polymer, extensively washed with water and MeOH, displayed an UV-Vis absorption spectrum with a slightly higher absorption with respect to that of the non-functionalized polymer (Fig. 12C, black line). To this functionalized polymer selective recognition experiments was carried out by using **1** (non-metallated form) and **2** (a schematic representation of the overall process is reported in Fig. 12A). In particular, THF solutions of **1** (non-metallated form) and **2** were placed over the **4**-GNPs functionalized polymer for 30 min. After this time, the solutions were removed and both polymeric matrices were washed several times with THF to remove the unbound **1** (non-metallated form) and **2**. As a result, the polymeric matrix changes in color (for **1** in its non-metallated form, see Fig. 12D). For both samples, solid-state UV-Vis absorption spectra were recorded, which demonstrated binding of **1** (in its non-metallated form, Fig. 12D, red line) and **2**.This last compound was reversibly isomerized directly on the surface by using light at 365 or 420 nm (Fig. 12E). As a control experiment, the direct absorption of **1** (non-metallated form) or **2** on the surface of the non-functionalized polymer did not take place in the absence of **4**-GNPs.

Conclusion

We have shown selective adenine-thymine binding occurring between complementary self-organized complex systems. These interactions result in precise supramolecular architectures that are morphologically dependent on the nature of the chromophore used. In particular, adenine

capped gold nanoparticles combined with *tetra*phenylporphyrin afforded supramolecular spherical aggregates, while combined with *azo*benzene generated straight fiber networks, further able to reorganize into bent fibre networks under *trans* to *cis* isomerization. The multifunctional nature of thymine-CQDs combined with adenine-capped GNPs generated an hybrid porous material which retained the characteristic electron-donating capabilities of the photoexcited pristine CQDs. Importantly, we successfully explored the self-shaping properties of the resulting microstructures by inducing a "shake-up" of supramolecular binding mode, promoted by the activation of the plasmon resonance of the adenine capped gold nanoparticles. In our view, the mixing process between adenine-GNPs and thymine-chromophores yields kinetic controlled microstructures, where all of the possible binding modes are cooperatively involved. Then, following the Vis-illumination (vibrational energy converted in heat propagation), the microstructures undergo to a H-bonding mode selections (including chromophore-chromophore interactions), that afford an ordered, self-shaped, morphological transition, morphologically dependent by the nature of the chromophores. We are currently investigating the nature of this interesting binding mode selection. Moreover, we successfully explored the selective binding at the surface level, proving spectroscopically its occurrence on a polymeric surface, where the adenine-capped GNPs were initially attached *via* a thiol-to-thiol exchange reactions and subsequently used as molecular sites for binding of thymine-functionalized *tetra*phenylporphyrin and *azo*benzene.

Supplementary Information (ESI) available: synthetic details and characterizations for all intermediates and final compounds **1**-**4**.

Acknowledgements

The authors thank Italian Ministry of University and Research (Futuro in Ricerca 2013, RBFR13RQXM) for financial support.

View Article Online
DOI: 10.1039/C6RA17673A

References

[1] A. R. Studart and R. M. Erb, *Soft Matter*, 2014, **10**, 1284-1294.

[2] J. M. Lehn, *Proc. Natl. Acad. Sci. USA*, 2002, **99**, 4763-4768.

[3] G. M. Whitesides and B. Grzybowski, *Science*, 2002, **295**, 2418-2421.

[4] J. F. Stoddart and H.-R. Tseng, *Proc. Natl. Acad. Sci. USA*, 2002, **99**, 4797-4800.

[5] E. Persch, O. Dumele and F. Diederich, *Angew. Chem. Int. Ed.,* 2015, **54**, 3290-3327.

[6] K. Ariga, H. Ito, J. P. Hill and H. Tsukube, *Chem. Soc. Rev.*, 2012, **41**, 5800-5835.

[7] G. Yu, K. Jie and F. Huang, *Chem. Rev.,* 2015, **115**, 7240-7303.

[8] A. K. Boal, F. Ilhan, J. E. DeRouchey, T. Thurn-Albrecht, T. P. Russell and V. M. Rotello, *Nature,* 2000, **404**, 746-748.

[9] E. Busseron, Y. Ruff, E. Moulin and N. Giuseppone, *Nanoscale*, 2013, **5**, 7098-7140.

[10] J. L. Sessler, C. M. Lawrence and J. Jayawickramarajah, *Chem. Soc. Rev.*, 2007, **36**, 314-325.

[11] S. Sivakova and S. J. Rowan, *Chem. Soc. Rev.*, 2005, **34**, 9-21.

[12] J. L. Sessler and J. Jayawickramarajah, *Chem. Commun.*, 2005, 1939-1949.

[13] L. Liu, D. Xia, L. H. Klausen and M. Dong, *Int. J. Mol. Sci.,* 2014, **15**, 1901-1914.

[14] A. Ciesielski, M. El Garah, S. Masiero and P. Samorì, *Small,* 2016, **12**, 83-95.

[15] W. Saenger, *Principles of Nucleic Acid Structures*, Springer, New York, 1984.

[16] A. G. Slater, Y. Hu, L. Yang, S. P. Argent, W. Lewis, M. O. Blunt and N. R. Champness, *Chem. Sci.*, 2015, **6**, 1562-1569.

[17] A. R. Fersht, *Trends Biochem. Sci*., 1987, **12**, 301-304.

[18] S. Choi, S. Park, S.-A. Yang, Y. Jeong and J. Yu, *Sci. Rep.,* 2015, **5**, 17805.

[19] L. Wang, S. J. Zhu, H. Y. Wang, S. N. Qu, Y. L. Zhang, J. H. Zhang, Q. D. Chen, H. L. Xu, W. Han, B. Yang and H. B. Sun, *ACS Nano*, 2014, **8**, 2541.

[20] A. R. Katritzky and T. Narindoshvili, *Org. Biomol. Chem.,* 2008, **6**, 3171-3176.

[21] K. L. Dueholm, M. Egholm, C. Behrens, L. Christensen, H. F. Hansen, T. Vulpius, K. H. Petersen, R. H. Berg, P. E. Nielsen and O. Buchardt, *J. Org. Chem.,* 1994, **59**, 5767-5773.

[22] K. Suzuki, L. Malfatti, D. Carboni, D. Loche, M. Casula, A. Moretto, M. Maggini, M. Takahashi and P. Innocenzi, *J. Phys. Chem. C,* 2015, **119**, 2837-2843.

[23] D. Mosconi, D. Mazzier, S. Silvestrini, A. Privitera, C. Marega, L. Franco, A. Moretto, *ACS Nano*, 2015, **9**, 4156-4164.

[24] D. Mazzier, M. Favaro, S. Agnoli, G. Granozzi, S. Silvetrini, M. Maggini, A. Moretto, *Chem. Commum.,* 2014, **50**, 6592-9595.

[25] M. Gouterman, *J. Mol. Spectrosc*., 1961, **6**, 138-163.

[26] G. Sudesh Kumar and D. C. Neckers, *Chem. Rev.,* 1989, **89,** 1915-1925.

[27] A. G. Slater, Y. Hu, L. Yang, S. P. Argent, W. Lewis, M. O. Blunt and N. R. Champness, *Chem. Sci.,* 2015, **6**, 1562-1569.

[28] W. Mamdouh, M. Dong, S. Xu, E. Rauls and F. Besenbacher, *J. Am. Chem. Soc.*, 2006, **128**, 13305-13311.

[29] Z. Wu, J. Suhana and R. Jin, *J. Mater. Chem.*, 2009, **19**, 622-626.

[30] E. Longo, A. Orlandin, F. Mancin, P. Scrimin and A. Moretto, *ACS Nano*, 2013, **7**, 9933-9939.

[31] P. D. Jadzinsky, G. Callero, C. J. Ackerson, D. A. Bushnell and R. D. Kornberg, *Science*, 2007, **318**, 430-433.

[32] S. Ogi, K. Sugiyasu, S. Manna, S. Samitsu and M. Takeuchi, *Nature Chem.,* 2014, **6**, 188-195.

[33] M. Schade, A. Moretto, P. Donaldson, C. Toniolo and P. Hamm, *Nanoletters*, 2010, **10**, 3057-3061.

View Article Online
DOI: 10.1039/C6RA17673A

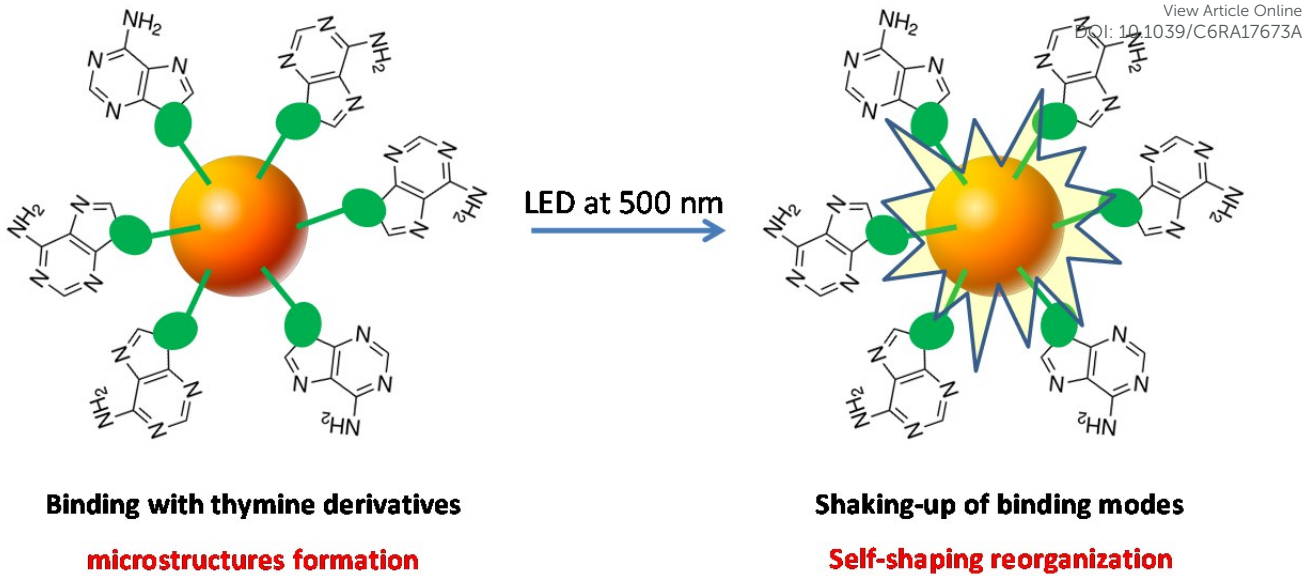

The selective adenine-thymine binding occurring between complementary self-organized complex systems can be modulated by the activation of the plasmon resonance.